Hindawi
Journal of Food Processing and Preservation
Volume 2023, Article ID 1400862, 13 pages
https://doi.org/10.1155/2023/1400862

Research Article

Isolation, Purification, Structural Characterization, and Hypoglycemic Activity of Polysaccharide from *Trichosanthes kirilowii* Maxim. Seed Shell

Qiaoying Song, Kunpeng Zhang, Lingbiao Gu, and Changlu Zhang

College of Biotechnology and Food Science, Anyang Institute of Technology, Huanghe Road, Anyang 455000, China

Correspondence should be addressed to Qiaoying Song; 969354025@qq.com

Received 27 February 2023; Revised 24 May 2023; Accepted 1 June 2023; Published 12 June 2023

Academic Editor: Prakash Bhuyar

In this manuscript, polysaccharide (TMSP) was isolated from *Trichosanthes kirilowii Maxim.* seed shell. The homogeneous polysaccharide (TMSP-1; molecular weight: 690.239 kDa) was purified by column chromatography (DEAE-cellulose-52 and Sephadex G-150). The result of monosaccharide composition showed that TMSP-1 consisted of D-mannose, D-glucose, D-galactose, and glucuronic acid in a molar ratio of 2.01 : 1.98 : 1.87 : 1. Methylation analysis showed that TMSP-1 was made up of →3)-D-Gal*p*-(1→, D-Glc*p*-(1→, →4)-D-Man*p*-(1→, →6)-D-Gal*p*-(1→, →4)-D-Gal*p*-(1→, and →4,6)-D-Man*p*-(1→. The microscopic conformation of TMSP-1 showed a regular flake-like structure that was inlaid with small holes. The α-glucosidase inhibitory rate of TMSP-1 reached 52.23% when the concentration of TMSP-1 was 8 mg/mL, which confirmed the potential hypoglycemic activity of TMSP-1 in vitro. In vivo results showed that type 2 diabetes causes a significant increase in organ index and TMSP-1 recovered the organ index in mice ($P < 0.05$). Furthermore, TMSP-1 reversed the increase of liver and kidney weight and the indicators of abnormality. This research lays a foundation for research on the polysaccharides of *Trichosanthes kirilowii Maxim.* seed shell in hypoglycemia.

1. Introduction

Trichosanthes kirilowii Maxim., a traditional Chinese herbal medicine, has received much attention from scholars because of its significant medicinal value [1]. Extracts from *T. kirilowii* are known to improve cardiovascular system function, can be used as a cough expectorant, and have anti-tumor and anti-inflammatory activities [2–4]. The seeds of *Trichosanthes kirilowii Maxim.* are edible and are rich in nutrients such as protein and oil. Research has shown that seeds are rarely classified as everyday consumer goods. But all kinds of plant seeds contain rich nutrients, such as polyphenols, flavonoids, and alkaloids. Therefore, more and more attention should be paid to plant seed nutrition and efficacy [5–8]. Modern medical studies have confirmed that *Trichosanthes kirilowii Maxim.* seeds contain unsaturated fatty acids, protein, amino acids, triterpene saponins, and 16 trace elements [5, 6]. Therefore, *Trichosanthes kirilowii Maxim.* seeds are also known as "drug homologous food," because they are widely used to treat cough and asthma, reduce phlegm, and treat other conditions [7, 8]. To date, the research on *Trichosanthes kirilowii Maxim.* seeds has mainly focused on their contents of flavonoids, essential oils, and protein [9–12]. Therefore, knowledge of the chemical constituents of *Trichosanthes kirilowii Maxim.* seeds is not yet comprehensive.

Polysaccharides are chains of sugars linked by glycosidic bonds and are generally composed of at least ten monosaccharide units [13]. It is well known that polysaccharides are widely distributed in nature because of their important physiological functions [14]. On the one hand, polysaccharide may exist as components of animal tissue and plant cell walls, such as peptidoglycan and cellulose [15]. On the other hand, polysaccharides have particular biological activities, such as hypoglycemic, antioxidation, antitumor, and antibacterial activities [16].

Diabetes mellitus (DM) is a clinical syndrome caused by the interaction of genetic and environmental factors [17].

Because of an absolute deficiency of insulin secretion, a series of metabolic disorders can occur involving imbalances in sugars, protein, fat, water, and electrolyte. DM can be divided into type 1 or type 2 diabetes [18]. Type 1 diabetes mostly occurs in young people and requires the administration of insulin to maintain life, whereas type 2 diabetes (T2DM) can occur at any age and can be controlled by oral hypoglycemic drugs. DM can cause many complications, such as nephropyelitis, urocystitis, and atherosclerotic cardiovascular disease [19]. Among them, diabetic nephropathy is one of the most common diseases. It is caused by hyperglycemia and is the main symptom of impaired renal structure and function. Clinical diabetic nephropathy is often associated with diabetic retinopathy, and almost all patients with diabetic nephrotic syndrome exhibit diabetic retinopathy. In addition, diabetes can also cause liver lesions, mainly manifested as cirrhosis [20].

Current studies of *Trichosanthes kirilowii Maxim.* seed have focused on the active components, such as flavonoids, proteins, and essential oils, while little research has been done on the polysaccharide of the seed. This study is aimed at exploring the structural character and hypoglycemic activity of polysaccharide isolated from *T. kirilowii* seed shell. The fine structure of polysaccharide was described, and its hypoglycemic activity on T2DM mice was evaluated. This study promotes a compelling reason to research on the polysaccharides of *Trichosanthes kirilowii Maxim.* seed shell in hypoglycemia.

2. Materials and Methods

2.1. Materials. *Trichosanthes kirilowii Maxim.* was provided by Anyang Institute of Technology. The Sephadex G-150 and DEAE-cellulose-52 were bought from Sigma Chemical Co. (USA). The standards of monosaccharides, such as D-glucose (D-Glc), D-xylose (D-Xyl), D-galactose (D-Gal), L-rhamnose (L-Rha), D-mannose (D-Man), and L-arabinose (L-Ara) were obtained from Solarbio (Beijing, China). The reagents used in HPGPC and GC-MS were of chromatographic grade. All other chemicals used in this study were of analytical grade.

Healthy male C57BL/6J mice (2-3 weeks, 20 ± 2 g) were purchased from Sibeifu Biotechnology Co., Ltd. (Beijing, China). Animal welfare and experimental procedures were carried out following the relevant laws and the Guide for the Care and Use of Laboratory Animals (Ministry of Science and Technology of China, 2006). None of the experiments involved human subjects.

2.2. Preparation of Polysaccharide. Polysaccharide was obtained by water extraction and alcohol precipitation [21]. *Trichosanthes kirilowii* seed shell was dried, ground to powder, and extracted with distilled water (1 : 60, *w*/*v*) [22]. The ethanol was added to aqueous supernatant to precipitate the crude polysaccharide (TMSP). Residual protein in the TMSP was removed with Sevag reagent. To obtain homogeneous polysaccharide (TMSP-1), the TMSP was purified by using DEAE-cellulose-52 and Sephadex G-150 (1.6×40 cm) [23].

2.3. Structural Analysis of TMSP-1

2.3.1. Molecular Weight (MW) Analysis of TMSP-1. The MW of TMSP-1 was determined by the method of Zhang et al. [24]. TMSP-1 and T-series dextrans (1 mg/mL) were analyzed by HPLC to calculate the MW of TMSP-1.

2.3.2. Fourier Transform Infrared (FT-IR) Analysis of TMSP-1. The analysis of FT-IR was operated according to the method of Zhang et al. [25]. The mixture of sample and dried KBr was prepared according to the literature. The FT-IR analysis of TMSP-1 was performed with FT-IR spectrophotometer (Perkin Elmer Corp., USA).

2.3.3. Monosaccharide Composition Analysis of TMSP-1. The degradation of TMSP-1 structure was referred to Song and Kong's method [26]. After the mixture of TMSP-1 solution (1 mL, 0.1 mg/mL) and trifluoroacetic acid (0.5 mL, 4 mol/L) was heated at 120°C for 2 h, PMP methanol solution (0.5 mL, 0.5 mol/L) and NaOH solution (0.5 mL, 0.3 mol/L) were added and heated in a water bath at 70°C for 30 min. After cooling to room temperature, the sample was neutralized with HCl solution (0.5 mL, 0.3 mol/L), and chloroform was used to remove organic impurities. The aqueous layer was filtered with a 0.22 μm membrane [27].

2.3.4. Methylation and Gas Chromatography-Mass Spectrometry of TMSP-1. The methylation of TMSP-1 was operated according to Heiss et al.'s method [28]. A mixture of dried TMSP-1 (20 mg) and NaH (100 mg) was added into anhydrous dimethyl sulfoxide (3 mL), heated at 28°C for 30 min. After the dropwise addition of CH_3I, the product was dialyzed and concentrated to dryness.

Trifluoroacetic acid solution (2 mL, 2 mol/L) was added to the methylated sample, which was then degraded for 3 h. The mixture was dried under N_2 to obtain the degradation products of fully methylated samples. Then, 25 mg of NaBH4 was added to the degradation product for reducing at room temperature in darkness. After the reaction, the methanol (3 mL) and acetic acid were added into the sample, and the mixture was evaporated to dryness. This process was repeated five times. After that, pyridine (1 mL) and acetic anhydride (1 mL) were added to the above-treated samples for acetylation. After the reaction, 1 mL of methanol was used to obtain the acetylated product. The acetylated product was dissolved in 2 mL of dichloromethane and then concentrated to about 1 mL with N_2 gas for analysis by gas chromatography-mass spectrometry.

2.3.5. Nuclear Magnetic Resonance (NMR) Spectroscopy of TMSP-1. Take 20 mg of polysaccharide sample, dissolve it in 0.5 ml of heavy water, load it into the NMR tube, and conduct detection using Bruker NMR spectrometer (400 MHz) [29].

2.3.6. Scanning Electron Microscopy (SEM) Analysis of TMSP-1. The fully dried polysaccharide sample was attached onto the sample stage using specialized double-sided tape, ensuring that the sample does not move or detach. Next, an ion sputtering coating machine was used to spray gold

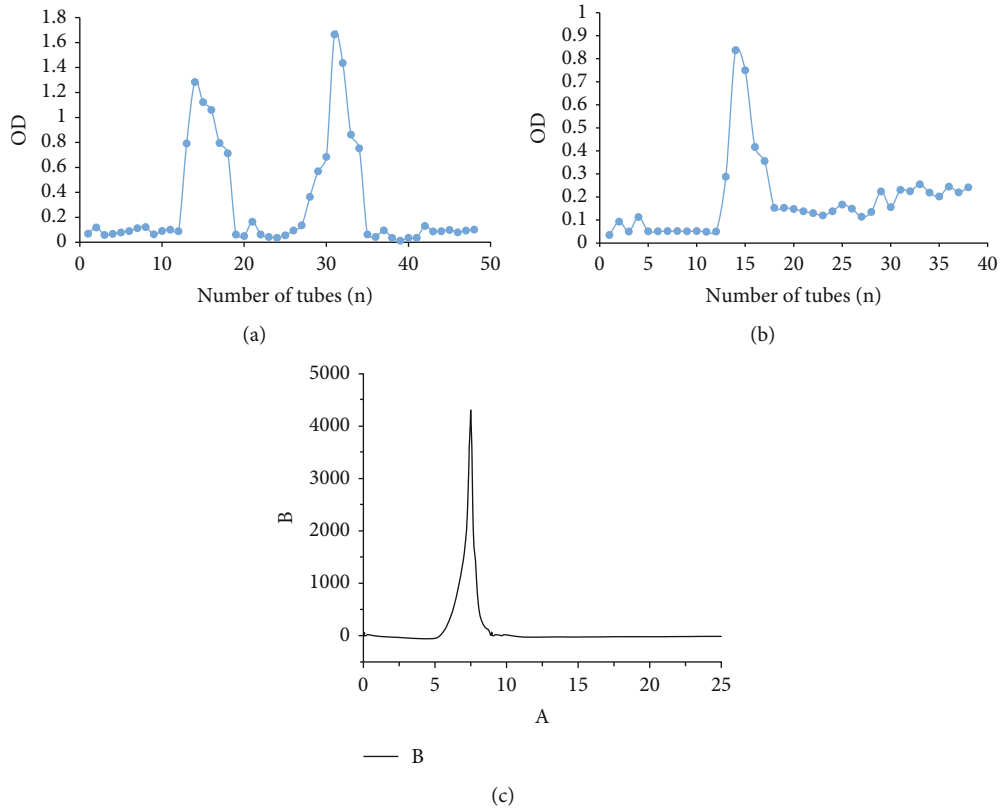

Figure 1: Elution results of DEAE-52 (a) and Sephadex G-150 (b) columns and the liquid chromatogram (c) of TMSP-1.

onto the sample surface. Finally, the gold-coated sample was placed into a scanning electron microscope and observe the morphology and structure of the sample at magnifications of 200-1000x [30].

2.4. α-Glucosidase Inhibitory Activity of TMSP-1. A 96-well microplate was used as a reaction carrier. In the sample group, α-glucosidase (yeast source, 40 U/mL) and TMSP-1 were added to each well. In the control group, an equal amount of TMSP-1 and phosphate buffer (0.1 mol/L, pH 6.8) was added to each well. In the blank group, equal amounts of α-glucosidase and phosphate buffer were added to each well. After the samples were incubated at 37°C for 10 min, 20 μL of *p*-nitrophenyl glucopyranoside (7.5 mmol/L) was added and the sample was incubated for a further 30 min. Na_2CO_3 solution (100 μL, 0.1 mol/L) was added into the sample to terminate the reaction. The inhibition rate was calculated as follows [12]:

$$\text{Inhibition rate} = \frac{A1 - A2}{A1 - A3} \times 100, \quad (1)$$

where $A1$ is the control group absorbance at 405 nm, $A2$ is the sample group absorbance at 405 nm, and $A3$ is the blank group absorbance at 405 nm.

2.5. Hypoglycemic Activity of TMSP-1 In Vivo

2.5.1. Design of Mouse Experiment. After 7 d of normal feeding, 10 C57BL/6J mice were randomly selected as the normal

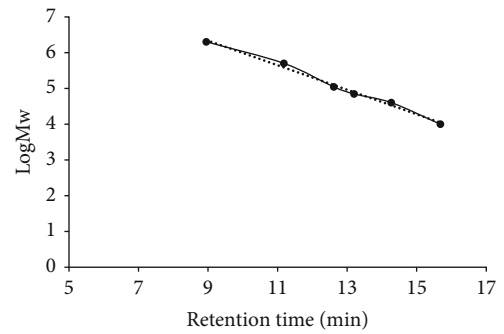

Figure 2: The calibration curve of *T*-series dextrans.

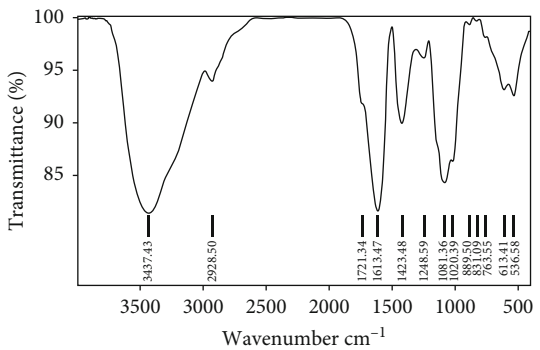

Figure 3: FT-IR spectrum of TMSP-1.

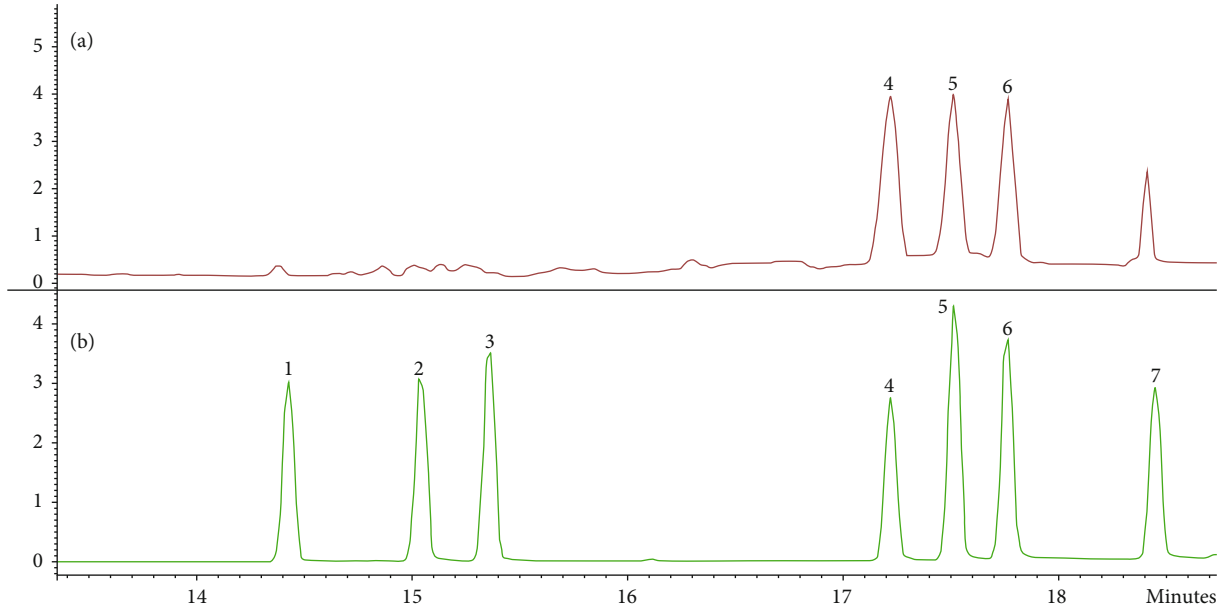

Figure 4: Monosaccharide composition analysis of (a) TMSP-1 and (b) 7 standard monosaccharides (1: L-rhamnose, 2: D-arabinose, 3: D-xylose, 4: D-mannose, 5: D-glucose, 6: D-galactose, and 7: glucuronic acid).

group (NG) and continued to be fed normally. After being fed a high-fat and sugar fodder for 4 weeks, the rest were injected with streptozotocin (STZ, intraperitoneal, 30 mg/kg) on day 3, after which feeding on high-fat and sugar fodder continued [28]. The NG group mice were injected with the same amount of saline solution and were fed basal fodder. Each mouse was fasted for 2 h after injection to ensure successful construction of the model. Three days after injection, blood samples were taken from the tail tip to measure blood glucose. The blood glucose range of 11.1–30 mmol/L indicated successful modeling. Otherwise, STZ was injected again at a dose of 25–40 mg/kg on the day after fasting until the modeling was successful [29].

The mice were randomly divided into the model group (MG) and the high- (H-TMSP-1), middle- (M-TMSP-1), and low-dose (L-TMSP-1) groups. Acarbose was used in the positive control group (PG). The mice in the NG group and MG group were fed with 0.9% saline solution (0.2 mL/10 g). The mice in the sample groups were fed with 100, 200, and 300 mg/kg bw of TMSP-1.

During feeding, the mice had free access to basic feed and water. The mice's fasting blood glucose (FBG) was recorded every 7 days. After 26 days of administration, the mice were fasted for 12 h. Each group of mice was given glucose (2.0 g/kg), and the blood glucose was measured at 0, 0.5, 1.0, 1.5, and 2.0 h. At 28 days after administration, serum was collected by eyeball extirpation. The liver and kidney were collected after dissection, and the organ index was measured [30].

2.5.2. Determination of Liver and Kidney Functional Indexes. Blood samples of the mice were collected before the mice were killed. Serum was obtained by centrifugation at 2000 rpm at 4°C for 20 min. The levels of aspartate aminotransferase (AST), albumin (ALB), blood urea nitrogen (BUN), and creatinine (CRE) were recorded using an automated biochemical analyzer. Insulin ELISA kit was used to detect serum insulin levels in each group.

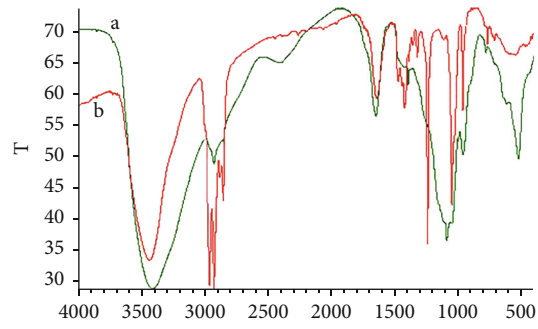

Figure 5: Infrared spectrum of TMSP-1 after methylation reaction: (a) infrared spectrum of TMSP-1 before methylation and (b) infrared spectrum of TMSP-1 after methylation.

2.5.3. Oxidative Stress Analysis. Mice's serum and organs were collected after the mice were killed. The activities of glutathione peroxidase (GSH-Px) and superoxide dismutase (SOD) and the content of malondialdehyde (MDA) were measured by insulin enzyme-linked immunosorbent assay.

2.6. Statistical Analysis. All samples were analyzed in triplicate and averaged; data were expressed as mean ± standard deviation (SD). Excel 2010 and Origin 2018 software were used for data processing and graphing.

Table 1: Results of the methylation analysis of TMSP-1.

	Methylation sugar residues	Linkage types	Major mass fragments (m/z)
a	2,4,6-Tri-O-Me_3-D-Gal	→3)-D-Gal*p*-(1→	43, 59, 87, 101, 113, 129, 142, 173, 187, and 205
b	2,3,4,6-Tetra-O-Me_4-D-Glu	D-Glc*p*-(1→	43, 45, 87, 101, 117, 131, 145, 159, and 205
c	2,3,6-Tera-O-Me_4-D-Man	→4)-D-Man*p*-(1→	43, 58, 87, 101, 117, 127, 143, 161, 201, 217, and 233
d	2,3,4-Tri-O-Me_3-D-Gal	→6)-D-Gal*p*-(1→	43, 87, 101, 113, 118, 129, 161, 173, 187, and 205
e	2,3,6-Tri-O-Me_3-D-Gal	→4)-D-Gal*p*-(1→	43, 45, 99, 103, 129, 161, 189, and 233
f	2,3-Di-O-Me_2-D-Man	→4,6)-D-Man*p*-(1→	43, 45, 117, 127, 201, and 261

3. Results

3.1. Isolation and Purification of Polysaccharides. After isolating crude polysaccharide, the homogeneous polysaccharide (TMSP-1) was obtained by column chromatography of the crude polysaccharide. The elution results of DEAE-52 and Sephadex G-150 columns and the liquid chromatogram of TMSP-1 are shown in Figure 1. As shown in Figure 1, there was a single symmetrical peak in the liquid chromatogram of TMSP-1, indicating that TMSP-1 was a single component [31]. In addition, the total sugar content of TMSP-1 was 98.67%, which suggested that TMSP-1 could be used for subsequent experiments.

3.2. Determination of MW of TMSP-1. The calibration curve of *T*-series dextrans (Figure 2) was established as follows: $y = -0.3652x + 8.962$ and $R^2 = 0.9928$ (y is the logMw and x is the retention time). From the retention time of TMSP-1 (7.32 min) (Figure 1(c)), the MW of TMSP-1 was calculated to be 690.239 kDa.

3.3. FT-IR Analysis of TMSP-1. The FT-IR spectrum of TMSP-1 (Figure 3) featured a strong absorption at 3437.7 cm^{-1}, indicating the presence of multiple -OH groups [32]. The C-H stretching vibration peak was located at 2928.5 cm^{-1} [33], that at 1613.4 cm^{-1} was assigned to the presence of C=H [34], and the three peaks at 1248.6, 1020.4, and 1081.4 cm^{-1} suggested the presence of pyranose [35]. After that, the peak at 1721.34 cm^{-1} was attributed the presence of alduronic acid. Moreover, the signal at 831.09 cm^{-1} indicated that α-glycosidic linkages was present in TMSP-1 [36].

3.4. Monosaccharide Composition Analysis of TMSP-1. As shown in Figure 4, the result of monosaccharide composition suggested that TMSP-1 was formed by D-mannose, D-glucose, D-galactose, and glucuronic acid in a molar ratio of 2.01 : 1.98 : 1.87 : 1.

3.5. Methylation Analysis of TMSP-1. The methylation reaction targets the free hydroxyl groups in the various monosaccharide residues, and the remaining hydroxyl groups indicate the junction position of the original monosaccharide residues [37]. Absorption peaks around 3500 cm^{-1} were usually detected by infrared spectroscopy to determine whether the methylated polysaccharide contains free hydroxyl group (-OH) [38]. As shown in Figure 5, the weakened peak at 3500 cm^{-1} illustrated that TMSP-1 was completely methylated [39].

The results of the methylation analysis of TMSP-1 showed that TMSP-1 was composed of →3)-D-Gal*p*-(1→, D-Glc*p*-(1→, →4)-D-Man*p*-(1→, →6)-D-Gal*p*-(1→, →4)-D-Gal*p*-(1→, and →4,6)-D-Man*p*-(1→ (Table 1), which were in accord with the results of monosaccharide composition analysis.

3.6. NMR Analysis of TMSP-1. As shown in Figure 6(a), the six different anomeric protons (5.56, 5.33, 5.29, 5.10, 4.97, and 4.86 ppm) in ^{1}H NMR spectrum of TMSP-1 confirmed that TMSP-1 was made up of six different types of glycosidic bond [40]. Furthermore, there also were six anomeric carbons (109.3, 106.05, 103.63, 102.83, 99.43, and 95.51 ppm) in ^{13}C NMR spectrum, which was in conformity with the interpretation of the ^{1}H NMR spectrum [41]. Moreover, the presence of a carbon resonance at 176.32 ppm showed that TMSP-1 was an acid polysaccharide [42], which was in conformity with the results of monosaccharide composition analysis. The signals at δ13.05/4.86 ppm confirmed the presence of →3)-D-Gal*p*-(1→ units [43], whereas those at δ101.69/4.69 ppm were attributed to the linkage of →4)-D-Man*p*-(1→ [44]. The signals at δ95.77/4.51 ppm and δ91.35/5.10 ppm were ascribed to D-Gcl*p*-(1→ and →6)-D-Gal*p*-(1→, respectively [45], and those at δ94.64/4.28ppm and δ101.98/4.32 ppm were assigned to →4)-D-Gal*p*-(1→ and →4,6)-D-Man*p*-(1→, respectively [46]. All of the conclusions drawn from the NMR spectra were consistent with the results of methylation analysis.

3.7. Scanning Electron Microscopy (SEM) Analysis of TMSP-1. The surface morphology of TMSP-1 is shown in Figure 7. The surface of the sample had an irregular flake-like structure and was inlaid with small holes. These structural features would be expected to provide a high surface area, thereby enhancing its biological activity.

3.8. α-Glucosidase Inhibitory Activity of TMSP-1. The α-glucosidase inhibitory activity of TMSP-1 is illustrated in Figure 8. Different concentrations of TMSP-1 exhibited different α-glucosidase inhibitory activities, indicating a dose-dependent inhibition. As the TMSP-1 concentration increased, the α-glucosidase inhibitory rate continued to increase. When the concentration of TMSP-1 reached 8 mg/mL, the inhibitory rate reached 52.23%. Therefore,

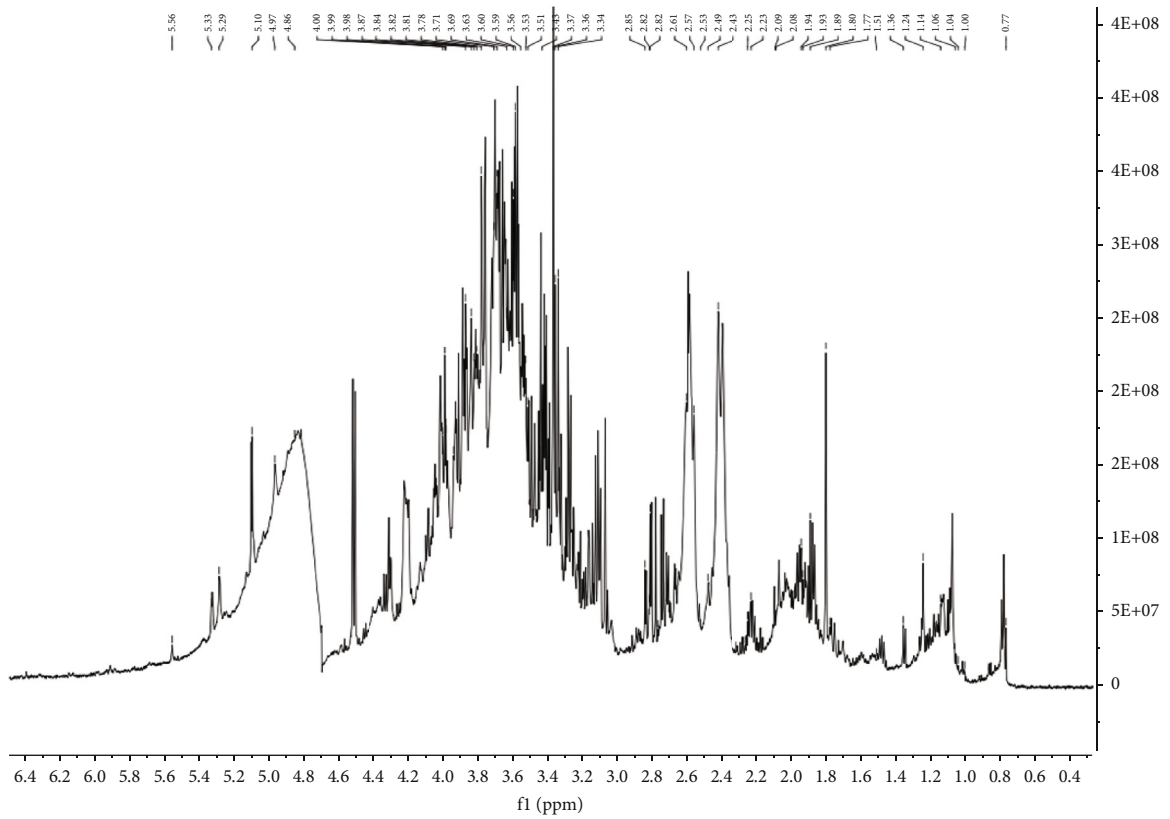

(a)

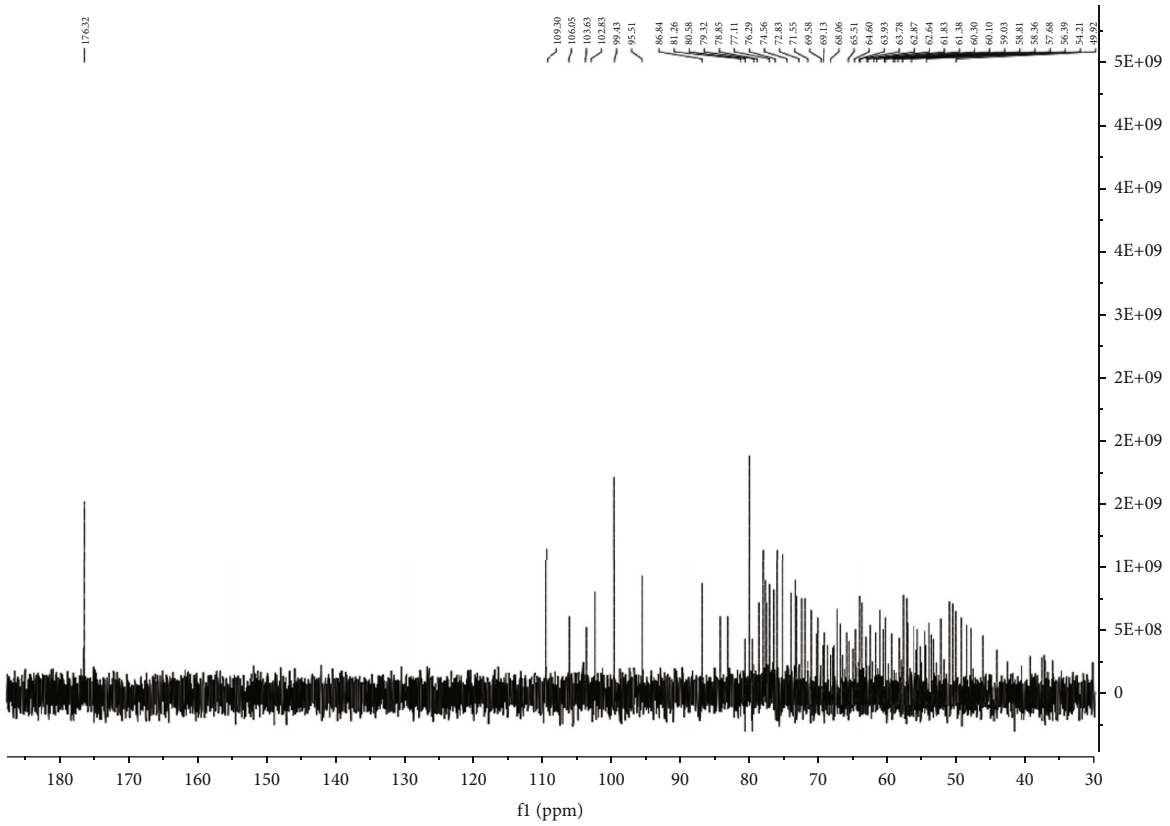

(b)

Figure 6: Continued.

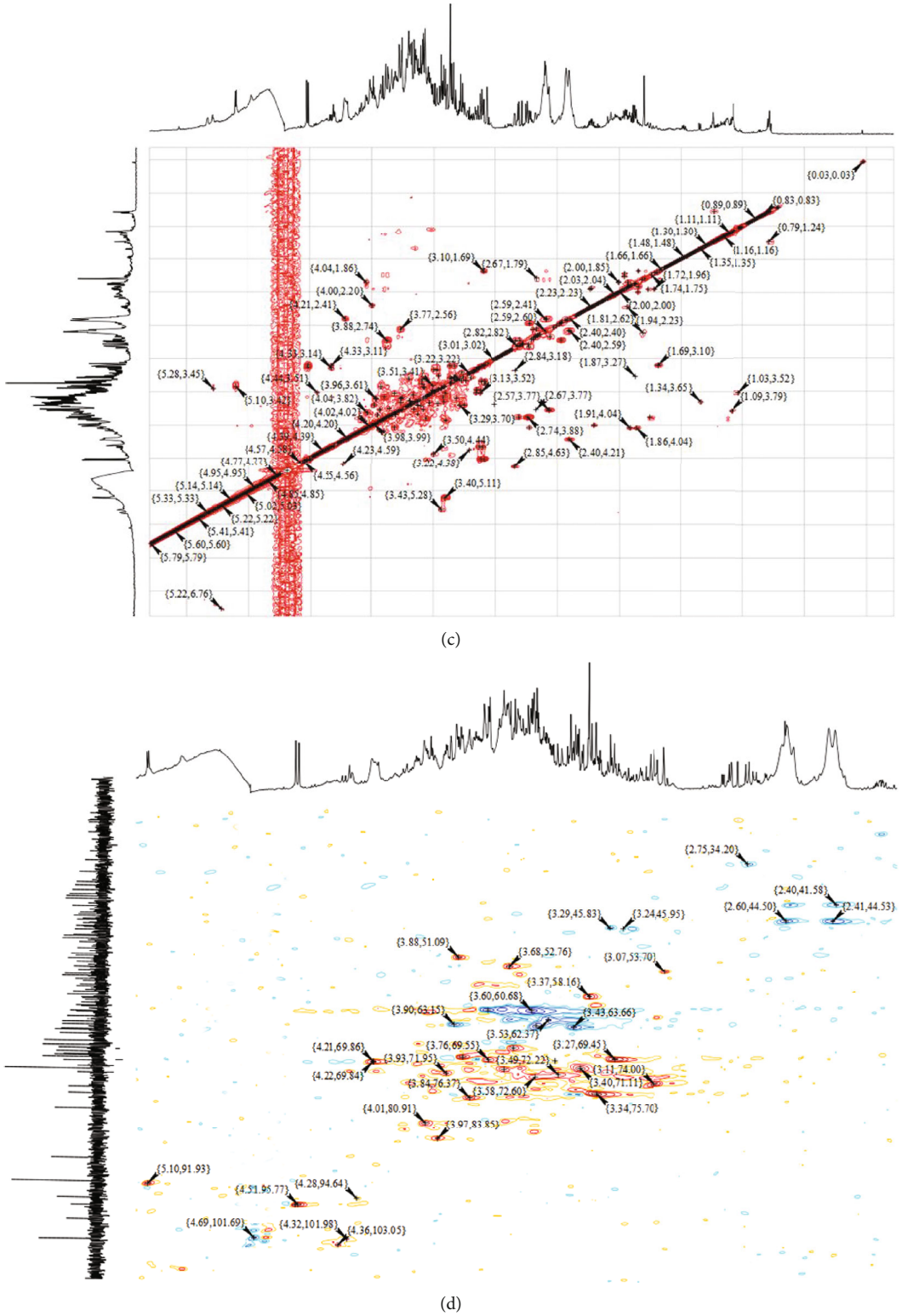

Figure 6: NMR analysis of TMSP-1: (a) ^{1}H NMR spectrum; (b) ^{13}C NMR spectrum; (c) COSY spectrum; (d) HSQC spectrum.

TMSP-1 has the potential for hypoglycemic activity in vitro. This is because TMSP-1 could prevent blood sugar from rising too quickly by inhibiting α-glucosidase activity, which slowed the digestion and absorption of carbohydrates and fats [47].

3.9. Organ Index Analysis. As presented in Table 2, the liver and kidney indexes in the MG group were significantly lower than those in the NG group ($P < 0.05$). Compared with the NG group, the liver and kidney indexes in the MG group were decreased by 39.9% and 68.2%, respectively, which

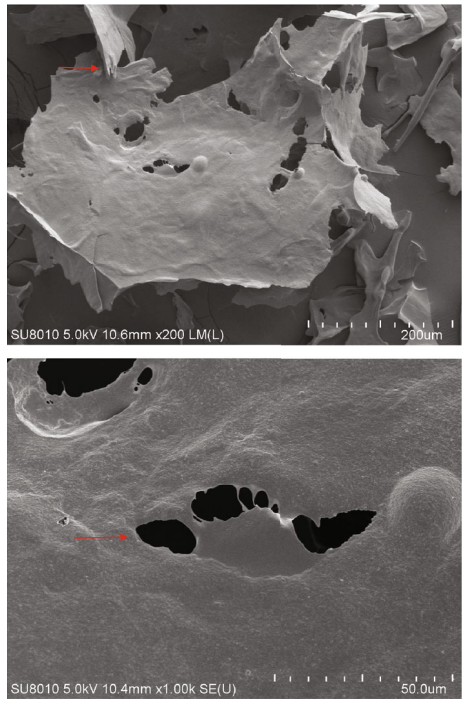

Figure 7: SEM analysis of TMSP-1.

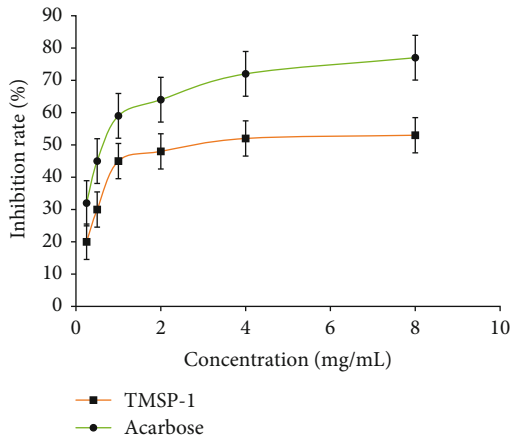

Figure 8: α-Glucosidase inhibitory activity of TMSP-1.

indicated the organ lesions in diabetic rats. After 4 weeks of TMSP-1 intervention, the liver and kidney indexes were apparently increased ($P < 0.05$).

In addition, the liver and kidney organ indexes in the H-TMSP-1 group were significantly different from those in the MG group ($P < 0.05$). The organ index was also observed to increase with increased dose of TMSP-1. The kidney index in the treatment groups showed no significant difference from the PG group ($P > 0.05$). Furthermore, we found a significant difference of liver index between the treatment groups and MG group ($P < 0.05$), except for the L-TMSP-1 group. In conclusion, this suggests that TMSP-1 could effectively improve organ health in T2DM mice.

3.10. Glycemic Index Analysis. The FBG levels of mice in each group were measured after fasting overnight. During the entire administration period, the FBG level of the NG group was maintained at 5 mmol/L. However, at the beginning of the experiment (0 week), the FBG level of the other groups was significantly higher than that in the NG group ($P < 0.01$), which indicated that STZ successfully induced and simulated a hyperglycemic model of diabetes in mice (Table 3). After 1st week and 2nd week of oral administrations of TMSP-1, we found that the FBG level decreased compared with the MG group, but the difference was not statistically significant ($P > 0.05$). However, after 3 weeks of administration, FBG level in the MG group was significantly higher than that in the PG group ($P < 0.01$). Compared with the MG group, FBG level in each administration group was significantly decreased ($P < 0.01$). In addition, after 3 weeks of administration, the FBG level in the M-TMSP-1 and H-TMSP-1 groups decreased by 25.34% and 42.31%, respectively ($P < 0.01$), which showed that TMSP-1 could control FBG level in T2DM mice.

3.11. Biochemical Assays of Serum. As we know, chronic high blood sugar can lead to diabetic kidney disease, such as nephrotic syndrome, which can lead to kidney failure or uremia in severe cases. As shown in Figures 9(a) and 9(b), the levels of CRE and BUN in the MG group were markedly higher than that in the NG group ($P < 0.01$), which showed that the kidney function of mice was obviously damaged. After 4 weeks of oral administrations of TMSP-1, the level of CRE and BUN in the TMSP-1 treatment groups was evidently and dose dependently reduced than that in the MG group ($P < 0.05$). These results indicated that TMSP-1 could ameliorate impaired kidney function by reducing the level of CRE and BUN.

As shown in Figures 9(c) and 9(d), the level of AST and ALB in the MG group was markedly higher than that in the NG group ($P < 0.01$). After 4 weeks of oral administrations of TMSP-1, the level of AST and ALB gradually approaches the NG group. Meanwhile, as the dose of TMSP-1 increased, the levels of AST and ALB showed decreasing trends, which suggested the relaxation effect of TMSP-1 by reducing the level of AST and ALB in serum.

3.12. Oxidative Stress Analysis. In the present study, the GSH-PX and SOD activities and MDA content in the liver and kidney were investigated to elevate the relationship between the occurrence of DM and oxidative stress. The obtained results (Figures 10(a) and 10(b)) showed that the activities of GSH-PX and SOD in the liver and kidney were significantly decreased, but MDA content increased compared with the NG group ($P < 0.01$), which suggested that DM could cause oxidative stress disorder in mice. After 4 weeks of oral administrations of TMSP-1, activities of GSH-PX and SOD in the liver and kidney were significantly increased with increased dose of TMSP-1. However, an opposing trend was observed for MDA content (Figure 10(c)), which indicated that TMSP-1 could attenuate oxidative stress by increasing antioxidant enzyme activity and inhibiting lipid peroxidation.

Table 2: The effect of TMSP-1 on liver and kidney organ indexes.

Index	NG group	MG group	PG group	L-TMSP-1	M-TMSP-1	H-TMSP-1
Liver	$5.26 \pm 0.36^{\#}$	$3.16 \pm 1.36^{*}$	$4.68 \pm 0.22^{\#}$	$3.25 \pm 0.43^{*}$	$4.25 \pm 1.02^{\#}$	$4.52 \pm 0.36^{\#}$
Kidney	$1.95 \pm 0.46^{\#}$	$0.62 \pm 0.08^{*}$	$1.16 \pm 0.15^{\#}$	0.88 ± 0.31	0.94 ± 0.06	$1.06 \pm 0.05^{\#}$

*Significantly different from the PG group ($P < 0.05$); $^{\#}$significantly different from the MG group ($P < 0.05$).

Table 3: Effect of TMSP-1 on blood glucose of T2DM mice.

Group	FBG (mmol/L)				
	0 days	7 days	14 days	21 days	28 days
NG group	$5.36 \pm 1.35^{**\#\#}$	$5.46 \pm 1.34^{**\#\#}$	$5.56 \pm 0.47^{**\#\#}$	$5.25 \pm 1.13^{**\#\#}$	$5.56 \pm 0.34^{**\#\#}$
MG group	26.48 ± 1.46	$25.56 \pm 1.24^{**}$	$24.24 \pm 3.24^{**}$	$25.24 \pm 4.23^{**}$	$25.34 \pm 1.42^{**}$
PG group	25.17 ± 1.63	$19.35 \pm 3.56^{\#\#}$	$16.24 \pm 4.34^{\#\#}$	$15.32 \pm 4.24^{\#\#}$	$14.35 \pm 4.24^{\#\#}$
L-TMSP-1	25.98 ± 0.68	$23.34 \pm 6.3^{**}$	$21.34 \pm 5.34^{**}$	$20.13 \pm 2.35^{**\#\#}$	$18.14 \pm 2.45^{**\#\#}$
M-TMSP-1	25.34 ± 1.05	$22.35 \pm 3.53^{**}$	$19.93 \pm 5.32^{**}$	$17.04 \pm 2.53^{**\#\#}$	$16.82 \pm 2.56^{**\#\#}$
H-TMSP-1	26.15 ± 1.35	$21.42 \pm 4.35^{**}$	$18.34 \pm 5.24^{**}$	$16.84 \pm 3.21^{**\#\#}$	$15.98 \pm 2.35^{**\#\#}$

*Significantly different from the PG group ($P < 0.05$); **extremely significantly different from the PG group ($P < 0.01$); $^{\#}$significantly different from the MG group ($P < 0.05$); $^{\#\#}$extremely significantly different from the MG group ($P < 0.01$).

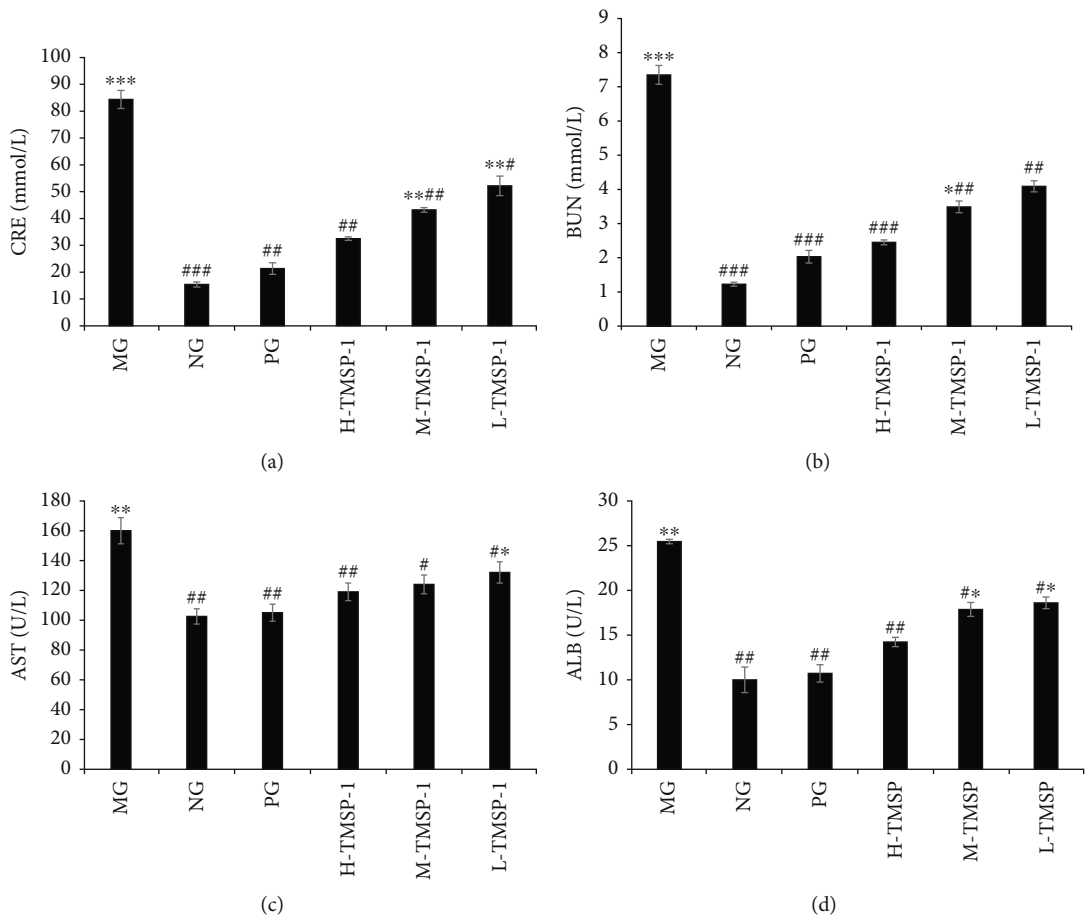

Figure 9: Effects of TMSP-1 on biochemical indices of serum: (a) CRE, (b) BUN, (c) AST, and (d) ALB; *: significantly different from the PG group ($P < 0.05$); **: extremely significantly different from the PG group ($P < 0.01$); #: significantly different from the MG group ($P < 0.05$); ##: extremely significantly different from the MG group ($P < 0.01$).

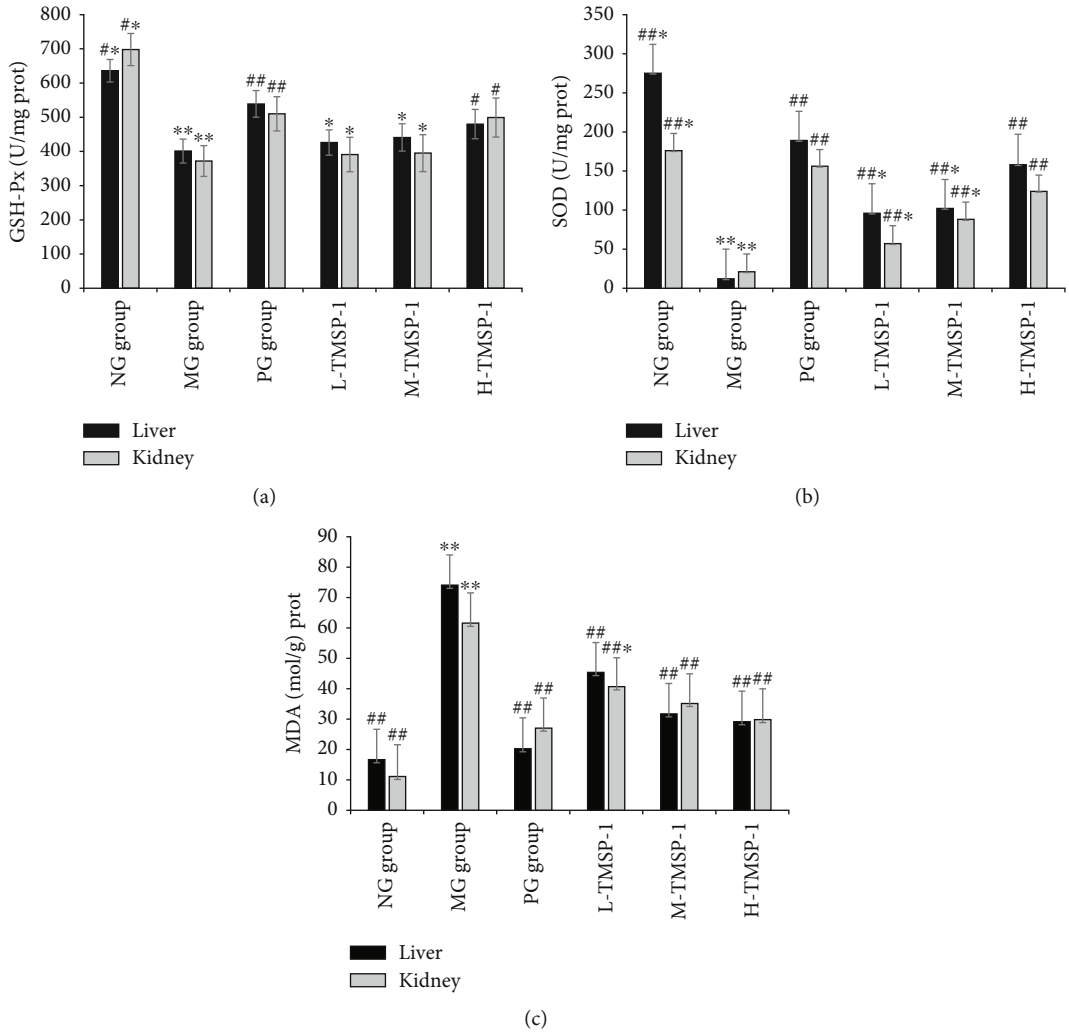

Figure 10: Effects of TMSP-1 on activities of SOD and GSH-Px and the concentrations of MDA in the liver and kidney: (a) GSH-Px, (b) SOD, and (c) MDA; *: significantly different from the control group ($P < 0.05$); #: significantly different from the model group ($P < 0.05$).

4. Discussion

DM is a metabolic disease characterized by hyperglycemia. With the improvement of living standards, the human lifestyle and dietary structure have also changed [48]. In recent years, diabetes has seriously endangered human health. At the same time, the treatment of diabetes proceeds mainly through insulin injection, oral hypoglycemic drugs, and diet therapy. However, prolonged use of these drugs causes inevitable toxic side effects to human health, which may easily lead to adverse reactions such as hypoglycemia, vomiting, and diarrhea [49].

Polysaccharides are natural macromolecules and one of the largest families of natural compounds. However, the analysis of polysaccharide structure is more complicated than the analysis of protein structure [50]. One factor contributing to such complexity is the abundance of monosaccharide types that make up polysaccharides (>200 known monosaccharides at present); the other factor relates to the branching structures of polysaccharides (proteins do not have branches). As a result, polysaccharide structures can be highly complex and difficult to characterize [51]. As we all know, polysaccharide is a kind of natural macromolecular compound with various biological activities, which has been proved to ameliorate the damage of the liver and kidney in diabetes mellitus.

In this study, we characterized the polysaccharide structure isolated from the seeds of *Trichosanthes kirilowii Maxim.* The result showed that TMSP-1 was composed of D-mannose, D-glucose, D-galactose, and glucuronic acid in a molar ratio of 2.01 : 1.98 : 1.87 : 1, which is consistent with the result of Sun et al. [52]. Analysis by methylation and NMR spectroscopy indicated that TMSP-1 was composed of →3)-D-Gal*p*-(1→, D-Glc*p*-(1→, →4)-D-Man*p*-(1→, →6)-D-Gal*p*-(1→, →4)-D-Gal*p*-(1→, and →4,6)-D-Man*p*-(1→.

The efficacy activity results suggested that TMSP-1 has hypoglycemic potential in vitro. In addition, there were significant decreases ($P < 0.05$) in the liver and kidney indexes in the MG group, which was consistent with the result of

Yang et al. [53]. Significant differences in organ index were observed among the MG group and treatment groups, which was consistent with the result of Jia et al. [54]. The loss of organ weight was caused by malnutrition brought about by insulin secretion [55]. Hyperglycemia has a complex relationship with oxidative stress. In addition, hyperglycemia induces the production of free radicals through a variety of molecular pathways [56]. As a kind of natural antioxidant, polysaccharide can reduce the damage caused by oxidative stress by improving the activity of antioxidant enzymes and removing free radicals in the body and ultimately improve the damage of diabetic liver and kidney. In this study, there were significant differences in GSH-PX and SOD activities and serum MDA between the MG group and treatment groups. Furthermore, increased doses of TMSP-1 pushed the activities of GSH-PX and SOD and MDA content closer to the respective values for the NG group, which was similar to the result of Liu et al. [57]. At the same time, patients with diabetes are often accompanied by dyslipidemia, such as elevated cholesterol and triglyceride levels. Polysaccharides can regulate lipid metabolism pathway, such as inhibiting cholesterol absorption and promoting fat decomposition, and maintain blood lipid generation in the body. Physicochemical indexes (AST, ALB, BUN, and CRE) are often used to measure the degree of organ damage caused by hyperglycemia. Previous studies have shown that hyperglycemia can cause liver and kidney injury [58]. Our study confirmed that TMSP-1 decreased the level of AST and ALB and increased the levels of BUN and CRE. This result was consistent with a previous study that showed that the polysaccharides from *Agrocybe cylindracea* could relieve the levels of physicochemical indexes [59]. Taken together, the results of the present study suggest that *T. kirilowii* can be used as a reference source for diabetes drug preparations.

5. Conclusion

In conclusion, a polysaccharide was obtained from *Trichosanthes kirilowii Maxim.* seed shell. The structure of polysaccharide was characterized with a variety of methods. The hypoglycemic activity of the polysaccharide was also performed in vitro and in vivo. All the results revealed that the polysaccharide was made up of →3)-D-Galp-(1→, D-Glcp-(1→, →4)-D-Manp-(1→, →6)-D-Galp-(1→, →4)-D-Galp-(1→, and →4,6)-D-Manp-(1→. At the same time, the polysaccharide has significant hypoglycemic activity. It provided the experimental basis and scientific support for the pharmacological application of *Trichosanthes kirilowii Maxim.*

Data Availability

The data used to support the findings of this study are included within the article.

Conflicts of Interest

The authors declare that they have no conflicts of interest.

Acknowledgments

This work was financially supported by the Staring Foundation for the Doctor, Anyang Institute of Technology (BSJ2021026); the Postdoctoral Innovation and Practice Base of Anyang Institute of Technology (BHJ2022010); and the Technological Program of Anyang, China (2021A01NY004 and 2022A02NY002).

References

[1] Z. R. Liang, D. W. Li, and S. M. Peng, "Effects of seed extracts from *Trichosanthes kirilowii* Maxim on antifeeding and growth and development of *Pieris rapae L*," *New Biotechnology*, vol. 25, p. S251, 2009.

[2] A. Abbou, N. Kadri, N. Debbache et al., "Effect of precipitation solvent on some biological activities of polysaccharides from *Pinus halepensis* Mill. seeds," *International Journal of Biological Macromolecules*, vol. 141, pp. 663–670, 2019.

[3] C. Fontes-Candia, L. Díaz-Piñero, J. Carlos Martínez, L. G. Gómez-Mascaraque, A. López-Rubio, and M. Martínez-Sanz, "Nanostructural changes in polysaccharide-casein gel-like structures upon in vitro gastrointestinal digestion," *Food Research International*, vol. 169, article 112862, 2023.

[4] S. Drouillard, L. Poulet, E. Marechal et al., "Structure and enzymatic degradation of the polysaccharide secreted by Nostoc commune," *Carbohydrate Research*, vol. 515, article 108544, 2022.

[5] S. Roy, T. Sarkar, and R. Chakraborty, "Vegetable seeds: a new perspective in future food development," *Journal of Food Processing and Preservation*, vol. 46, no. 11, article 17118, 2022.

[6] S. S. Moon, A. A. Rahman, J. Y. Kim, and S. H. Kee, "Hanultarin, a cytotoxic lignan as an inhibitor of actin cytoskeleton polymerization from the seeds of Trichosanthes kirilowii," *Bioorganic & Medicinal Chemistry*, vol. 16, no. 15, pp. 7264–7269, 2008.

[7] T. Sarkar, M. Salauddin, A. Roy et al., "Minor tropical fruits as a potential source of bioactive and functional foods," *Food Science & Nutrition*, pp. 1–45, 2022.

[8] S. H. Shu, G. Z. Xie, X. L. Guo, and M. Wang, "Purification and characterization of a novel ribosome-inactivating protein from seeds of Trichosanthes kirilowii Maxim," *Protein Expression and Purification*, vol. 67, no. 2, pp. 120–125, 2009.

[9] H. Liu, W. Kwame Amakye, and J. Ren, "Codonopsis pilosula polysaccharide in synergy with dacarbazine inhibits mouse melanoma by repolarizing M2-like tumor-associated macrophages into M1-like tumor-associated macrophages," *Biomedicine & Pharmacotherapy*, vol. 142, article 112016, 2021.

[10] Y. Sun, X. Hu, and W. Li, "Antioxidant, antitumor and immunostimulatory activities of the polypeptide from Pleurotus eryngii mycelium," *International Journal of Biological Macromolecules*, vol. 97, pp. 323–330, 2017.

[11] X. L. Ji, J. H. Guo, T. Z. Cao, T. Zhang, Y. Liu, and Y. Yan, "Review on mechanisms and structure-activity relationship of hypoglycemic effects of polysaccharides from natural resources," *Food Science and Human Wellness*, vol. 12, no. 6, pp. 1969–1980, 2023.

[12] A. C. Ruthes, F. R. Smiderle, and M. Iacomini, "Mushroom heteropolysaccharides: a review on their sources, structure and biological effects," *Carbohydrate Polymers*, vol. 136, pp. 358–375, 2016.

[13] Z. Ren, J. Li, N. Xu et al., "Anti-hyperlipidemic and antioxidant effects of alkali-extractable mycelia polysaccharides by Pleurotus eryngii var. tuolensis," *Carbohydrate Polymers*, vol. 175, pp. 282–292, 2017.

[14] Y. Sun, Z. Zhang, L. Cheng et al., "Polysaccharides confer benefits in immune regulation and multiple sclerosis by interacting with gut microbiota," *Food Research International*, vol. 149, article 110675, 2021.

[15] S. Richards, J. Dawson, and M. Stutter, "The potential use of natural vs commercial biosorbent material to remediate stream waters by removing heavy metal contaminants," *Journal of Environmental Management*, vol. 231, pp. 275–281, 2019.

[16] D. Chen, X. Liu, R. Bian et al., "Effects of biochar on availability and plant uptake of heavy metals: a metaanalysis," *Journal of Environmental Management*, vol. 222, pp. 76–85, 2018.

[17] M. Mleczek, M. Siwulski, P. Rzymski et al., "Comparison of elemental composition of mushroom Hypsizygus marmoreus originating from commercial production and experimental cultivation," *Scientia Horticulturae*, vol. 236, pp. 30–35, 2018.

[18] M. Liu, W. Yao, Y. Zhu, H. Liu, J. Zhang, and L. Jia, "Characterization, antioxidant and antiinflammation of mycelia selenium polysaccharides from Hypsizygus marmoreus SK-03," *Carbohydrate Polymers*, vol. 201, pp. 566–574, 2018.

[19] L. Yang, Z. Wang, and L. Huang, "Isolation and structural characterization of a polysaccharide FCAP1 from the fruit of Cornus officinalis," *Carbohydrate Research*, vol. 345, no. 13, pp. 1909–1913, 2010.

[20] Q. Song, T. Li, W. Xue et al., "Preparation, structure analysis and ACE inhibitory activity of konjac oligosaccharide," *Industrial Crops and Products*, vol. 124, pp. 812–821, 2018.

[21] Q. Song, L. Gu, H. Wu, S. Ma, L. Kong, and K. Zhang, "Chemical structure and ACE inhibitory activity of polysaccharide from *Artemisia vulgaris L.*," *Journal of Molecular Structure*, vol. 1250, article 131896, 2022.

[22] J. Li and G. Huang, "Extraction, purification, separation, structure, derivatization and activities of polysaccharide from Chinese date," *Process Biochemistry*, vol. 110, pp. 231–242, 2021.

[23] W. He, R. Pan, L. Li et al., "Combined lowering effect of phytosterol esters and tea extracts on lipid Profiles in SD rats," *Food Science and Technology Research*, vol. 24, no. 5, pp. 875–882, 2018.

[24] X. Zhang, X. Kong, Y. Hao, X. Zhang, and Z. Zhu, "Chemical structure and inhibition on α-glucosidase of polysaccharide with alkaline-extracted from Glycyrrhiza inflata residue," *International Journal of Biological Macromolecules*, vol. 147, pp. 1125–1135, 2020.

[25] G. Zhang, Q. Yin, T. Han et al., "Purification and antioxidant effect of novel fungal polysaccharides from the stroma of *Cordyceps kyushuensis*," *Industrial Crops and Products*, vol. 69, pp. 485–491, 2015.

[26] Q. Song and L. Kong, "Chemical structure and protective effect against alcoholic kidney and heart damages of a novel polysaccharide from Piperis Dahongpao," *Carbohydrate Research*, vol. 522, article 108698, 2022.

[27] J. Yan, L. Zhu, Y. Qu et al., "Analyses of active antioxidant polysaccharides from four edible mushrooms," *International Journal of Biological Macromolecules*, vol. 123, pp. 945–956, 2019.

[28] C. Heiss, I. Black, M. Ishihara, M. Tatli, T. P. Devarenne, and P. Azadi, "Structure of the polysaccharide sheath from the B race of the green microalga Botryococcus braunii," *Algal Research*, vol. 55, article 102252, 2021.

[29] X. Liu, L. Wang, C. Zhang, H. Wang, X. Zhang, and Y. Li, "Structure characterization and antitumor activity of a polysaccharide from the alkaline extract of king oyster mushroom," *Carbohydrate Polymers*, vol. 118, pp. 101–106, 2015.

[30] D. Zeng and S. Zhu, "Purification, characterization, antioxidant and anticancer activities of novel polysaccharides extracted from *Bachu mushroom*," *International Journal of Biological Macromolecules*, vol. 107, pp. 1086–1092, 2018.

[31] S. P. Kim, S. O. Park, S. J. Lee, S. H. Nam, and M. Friedman, "A polysaccharide isolated from the liquid culture of *Lentinus edodes (shiitake)* mushroom mycelia containing black rice bran protects mice against a Salmonella Lipopolysaccharide-Induced Endotoxemia," *Journal of Agricultural and Food Chemistry*, vol. 61, no. 46, pp. 10987–10994, 2013.

[32] X. Liu, Z. Zhu, Y. Tang et al., "Structural properties of polysaccharides from cultivated fruit bodies and mycelium of Cordyceps militaris," *Carbohydrate Polymers*, vol. 142, pp. 63–72, 2016.

[33] J. Chen, T. Zhang, B. Jiang, W. Mu, and M. Miao, "Characterization and antioxidant activity of Ginkgo biloba exocarp polysaccharides," *Carbohydrate Polymers*, vol. 87, no. 1, pp. 40–45, 2012.

[34] Y. Chen and Y. Xue, "Purification, chemical characterization and antioxidant activities of a novel polysaccharide from Auricularia polytricha," *International Journal of Biological Macromolecules*, vol. 120, no. Part A, pp. 1087–1092, 2018.

[35] Y. Wang, N. Liu, X. Xue, Q. Li, D. Sun, and Z. Zhao, "Purification, structural characterization and in vivo immunoregulatory activity of a novel polysaccharide from *Polygonatum sibiricum*," *International Journal of Biological Macromolecules*, vol. 160, pp. 688–694, 2020.

[36] X. Song, Z. Feng, J. Tan, Z. Wang, and W. Zhu, "Dietary administration of *Pleurotus ostreatus* polysaccharides (POPS) modulates the non-specific immune response and gut microbiota diversity of *Apostichopus japonicus*," *Aquaculture Reports*, vol. 19, article 100578, 2021.

[37] C. Su, D. Fan, L. Pan, Y. Lu, Y. Wang, and M. Zhang, "Effects of Yu-Ping-Feng polysaccharides (YPS) on the immune response, intestinal microbiota, disease resistance and growth performance of Litopenaeus vannamei," *Fish & Shellfish Immunology*, vol. 105, pp. 104–116, 2020.

[38] F. Wang, S. Ye, Y. Ding et al., "Research on structure and antioxidant activity of polysaccharides from Ginkgo biloba leaves," *Journal of Molecular Structure*, vol. 1252, article 132185, 2022.

[39] Y. Ge, Y. Duan, G. Fang, Y. Zhang, and S. Wang, "Polysaccharides from fruit calyx of Physalis alkekengi var. francheti: isolation, purification, structural features and antioxidant activities," *Carbohydrate Polymers*, vol. 77, no. 2, pp. 188–193, 2009.

[40] B. Li, N. Zhang, Q. Feng et al., "The core structure characterization and of ginseng neutral polysaccharide with the immune-enhancing activity," *International Journal of Biological Macromolecules*, vol. 123, pp. 713–722, 2019.

[41] L. Zhang, Y. Hu, X. Duan et al., "Characterization and antioxidant activities of polysaccharides from thirteen boletus mushrooms," *International Journal of Biological Macromolecules*, vol. 113, pp. 1–7, 2018.

[42] Y. Wang, F. Wang, X. Ma et al., "Extraction, purification, characterization and antioxidant activity of polysaccharides from Piteguo fruit," *Industrial Crops and Products*, vol. 77, pp. 467–475, 2015.

[43] X. Xiang, R. Wang, H. Chen et al., "Structural characterization of a novel marine polysaccharide from mussel and its antioxidant activity in RAW264.7 cells induced by H_2O_2," *Bioscience*, vol. 47, article 101659, 2022.

[44] H. Tian, H. Liu, W. Song et al., "Structure, antioxidantand immunostimulatory activities of the polysaccharides from Sargassum carpophyllum," *Algal Research*, vol. 49, article 101853, 2020.

[45] F. Huang, R. Zhang, Y. Liu et al., "Characterization and mesenteric lymph node cells-mediated immunomodulatory activity of litchi pulp polysaccharide fractions," *Carbohydrate Polymers*, vol. 152, pp. 496–503, 2016.

[46] Y. Guo, X. Chen, and P. Gong, "Classification, structure and mechanism of antiviral polysaccharides derived from edible and medicinal fungus," *International Journal of Biological Macromolecules*, vol. 183, pp. 1753–1773, 2021.

[47] M. Siwińska, A. Zabłotni, E. Levina et al., "The unique structure of bacterial polysaccharides - Immunochemical studies on the O-antigen of Proteus penneri 4034-85 clinical strain classified into a new O83 *Proteus* serogroup," *International Journal of Biological Macromolecules*, vol. 163, pp. 1168–1174, 2020.

[48] P. Javed and P. K. Mandal, "Bacterial surface capsular polysaccharides from Streptococcus pneumoniae: a systematic review on structures, syntheses, and glycoconjugate vaccines," *Carbohydrate Research*, vol. 502, article 108277, 2021.

[49] N. Li, C. Wang, M. Georgiev et al., "Advances in dietary polysaccharides as anticancer agents: structure-activity relationship," *Trends in Food Science & Technology*, vol. 111, pp. 360–377, 2021.

[50] N. Li, C. Yan, D. Hua, and D. Zhang, "Isolation, purification, and structural characterization of a novel polysaccharide from Ganoderma capense," *International Journal of Biological Macromolecules*, vol. 57, pp. 285–290, 2013.

[51] M. Xu, T. Yan, G. Gong et al., "Purification, structural characterization, and cognitive improvement activity of a polysaccharides from Schisandra chinensis," *International Journal of Biological Macromolecules*, vol. 163, pp. 497–507, 2020.

[52] Y. Sun, C. Zhang, P. Zhang, C. Ai, and S. Song, "Digestion characteristics of polysaccharides from Gracilaria lemaneiformis and its interaction with the human gut microbiota," *International Journal of Biological Macromolecules*, vol. 213, pp. 305–316, 2022.

[53] Z. M. Yang, Y. Wang, and S. Y. Chen, "*Astragalus* polysaccharide alleviates type 2 diabetic rats by reversing the glucose transporters and sweet taste receptors/GLP-1/GLP-1 receptor signaling pathways in the intestine-pancreatic axis," *Journal of Functional Foods*, vol. 76, article 104310, 2021.

[54] R. B. Jia, Z. R. Li, J. Wu et al., "Physicochemical properties of polysaccharide fractions from Sargassum fusiforme and their hypoglycemic and hypolipidemic activities in type 2 diabetic rats," *International Journal of Biological Macromolecules*, vol. 147, pp. 428–438, 2020.

[55] Q. Wang, Y. Zheng, W. Zhuang, X. Lu, X. Luo, and B. Zheng, "Genome-wide transcriptional changes in type 2 diabetic mice supplemented with lotus seed resistant starch," *Food Chemistry*, vol. 264, pp. 427–434, 2018.

[56] H. Yaribeygi, S. L. Atkin, and A. Sahebkar, "A review of the molecular mechanisms of hyperglycemia-induced free radical generation leading to oxidative stress," *Journal of Cellular Physiology*, vol. 234, no. 2, pp. 1300–1312, 2019.

[57] Y. P. Liu, Y. M. Li, W. L. Zhang, M. Sun, and Z. Zhang, "Hypoglycemic effect of inulin combined with ganoderma lucidum polysaccharides in T2DM rats," *Journal of Functional Foods*, vol. 55, pp. 381–390, 2019.

[58] T. Xia, C. S. Liu, Y. N. Hu et al., "Coix seed polysaccharides alleviate type 2 diabetes mellitus via gut microbiota-derived short-chain fatty acids activation of IGF1/PI3K/AKT signaling," *Food Research International*, vol. 150, no. Part A, article 110717, 2021.

[59] W. X. Sun, Y. H. Zhang, and L. Jia, "Polysaccharides from Agrocybe cylindracea residue alleviate type 2-diabetes-induced liver and colon injuries by p38 MAPK signaling pathway," *Bioscience*, vol. 47, article 101690, 2022.